Analytical and experimental study of two delay-coupled excitable units

Lionel Weicker and Thomas Erneux
Université Libre de Bruxelles, Optique Nonlinéaire Théorique, Campus Plaine, C. P. 231, 1050 Bruxelles, Belgium

Lars Keuninckx and Jan Danckaert
Applied Physics Research Group (APHY), Vrije Universiteit Brussel, 1050 Brussel, Belgium

(Received 28 July 2013; published 9 January 2014)

We investigate the onset of time-periodic oscillations for a system of two identical delay-coupled excitable (nonoscillatory) units. We first analyze these solutions by using asymptotic methods. The oscillations are described as relaxation oscillations exhibiting successive slow and fast changes. The analysis highlights the determinant role of the delay during the fast transition layers. We then study experimentally a system of two coupled electronic circuits that is modeled mathematically by the same delay differential equations. We obtain quantitative agreements between analytical and experimental bifurcation diagrams.

DOI: 10.1103/PhysRevE.89.012908 PACS number(s): 05.45.Xt, 02.30.Ks, 87.19.lm

I. INTRODUCTION

Complex firing patterns are believed to play a critical role in many brain functions. Individual neurons may show irregular behavior [1], while ensembles of different neurons can synchronize in order to process biological information [2] or to produce regular, rhythmical activity [3]. The rhythms depend on the dynamical properties of each individual cell, the nature of the connections between neurons, and the network architecture. Anomalous forms of synchronization have been connected to sensory processing disorders, sleep alterations, parkinsonian tremor, and motor neuron diseases. A minimal model consisting of two coupled FitzHugh-Nagumo (FHN) units is the starting point of many studies on electrically coupled neural systems [4–6]. The FHN model is a slow-fast system of two coupled ordinary differential equations that extracts the essential dynamical behavior of more complex systems of equations modeling neurons. Here, we exclusively consider the excitable (nonoscillatory) FHN system. It admits a single steady state that is always linearly stable but a slight perturbation above threshold may initiate a large pulse of activity.

During the past decade, researchers became interested by the effects of communication time delays between coupled neurons [7,8]. Systematic numerical simulations of two mutually delayed-coupled excitable FHN systems [9–12] have shown that a stable periodic regime is possible as an alternative to a stable steady state. The two units oscillate in antiphase and the delay needs to surpass a critical value. There are no oscillations if the delay is zero. In the amplitude versus delay bifurcation diagram, a saddle-node bifurcation of limit cycles is responsible for the generation of stable oscillations. Physically, these oscillations are seen as a new form of synchronization that could reinforce the coherence of the network [13,14]. The emergence of isolated branches of periodic solutions for systems described by delay differential equations is an important dynamical phenomenon that deserves more attention [15]. It motivates our analytical investigation of the two coupled FHN system.

In [11], the following FHN equations,

$$\varepsilon\frac{dx_j}{dt} = -y_j + x_j - \frac{x_j^3}{3} + C[x_{3-j}(t-\tau) - x_j], \qquad (1)$$

$$\frac{dy_j}{dt} = x_j + a \quad (j = 1,2), \qquad (2)$$

were investigated where ε is a small parameter. The authors found numerically nearly 2τ-periodic solutions consisting of two slowly varying plateaus for x_1 and x_2 connected by fast transition layers. Approximations for the slow parts of the periodic solution can be constructed without difficulties. But the analysis of the fast transition layers is much more subtle. Specifically, it requires the solution of the following nonlinear differential equation

$$\frac{dx}{ds} = -y_0 + x - \frac{x^3}{3} + C[x(s+\delta) - x], \qquad (3)$$

where $s \equiv t/\varepsilon$. The constants y_0 and δ are unknown and are determined by seeking a solution of Eq. (3) satisfying boundary conditions at $s = \pm\infty$. The quantity $\varepsilon\delta$ is called "turn-on delay" in [11] and is defined as the small correction of the period from its leading value $T = 2\tau$. The presence of the time lag δ in Eq. (3) excludes any hope to find an analytical solution. In order to explore the role of these transition layers, we consider a piecewise linear FHN problem that allows analytical solutions. As we shall demonstrate, the solution of the transition layer equations are needed for the bifurcation diagram of the periodic solutions. Specifically, we introduce the following FHN equations:

$$\varepsilon\frac{dx_j}{dt} = -y_j - x_j + H[x_{3-j}(t-\tau) - a], \qquad (4)$$

$$\frac{dy_j}{dt} = x_j \quad (j = 1,2), \qquad (5)$$

where $H(x)$ is the Heaviside function, $0 < a < 1/2$ is the threshold parameter for excitability, $\varepsilon \ll 1$ is a small parameter, and $\tau = O(1)$ is the delay of the feedback. Equations (4) and (5) have been used for other neuronal systems exhibiting a delayed feedback [16,17]. The main advantage of Eqs. (4) and (5) compared to Eqs. (1) and (2) is that the transition layer equations become linear ordinary differential equations that we can solve.

For mathematical clarity, we concentrate on the periodic solution of Eqs. (4) and (5) where the two units oscillate in antiphase and are nearly 2τ periodic in time. In-phase

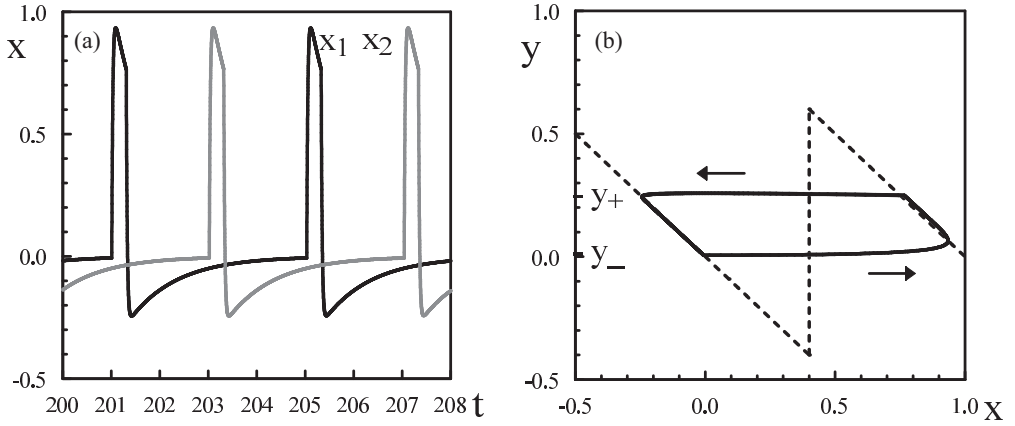

FIG. 1. (a) Antiphase oscillations. The values of the parameters are $\varepsilon = 0.02$, $a = 0.4$, and $\tau = 2$. (b) Phase-plane orbits for (x_1, y_1) and (x_2, y_2). Both orbits follow two branches of the function $y = -x + H(x - a)$ (broken line) connected by fast transition layers localized close to $y = y_- \simeq 0.062$ and $y = y_+ \simeq 0.25$.

periodic solutions or coexisting periodic solutions of different period are possible and they can be analyzed using the same asymptotic approach. They are briefly shown in the Discussion section.

How robust are the 2τ-periodic regimes with respect to noise? In the second part of the paper, we explore the response of two coupled electronic circuits that are described mathematically by the same FHN equations. These experiments are not a routine investigation of an electronic system because a high precision is needed to measure the turn-on delay $\varepsilon\delta$.

In Sec. II, we determine separate approximations for the slow and fast parts of the oscillations valid in the limit ε small. By combining each approximation over a period, we obtain bifurcation equations that we analyze using either τ or a as the control parameter. In Sec. III, we describe the experiments in detail and determine a bifurcation diagram with a as the control parameter (τ fixed). We then compare our experimental results with our theoretical predictions and obtain good quantitative agreements between the different bifurcation diagrams. Finally, we discuss our results in Sec. IV.

II. THEORY

Equations (4) and (5) admit only one steady-state solution $(x_j, y_j) = (0,0)$. This state is always stable but under specific initial conditions and parameter values a stable time-periodic solution where $x_1(t)$ and $x_2(t)$ oscillate in antiphase is possible. See Fig. 1(a). We observe that the period of the oscillations is close to $T = 4$ which suggests that $T \simeq 2\tau$ in first approximation, since $\tau = 2$. We also note that the behavior of the solution can be decomposed into two slowly varying parts and two fast transitions layers. Figure 1(b) represents the periodic solution in the phase plane. Both (x_1, y_1) and (x_2, y_2) exhibit the same orbit. The slowly varying parts of the solution can be described by taking advantage of the small value of ε. Indeed, inserting $\varepsilon = 0$ into Eq. (4) leads to the functions

$$y = 1 - x \quad (x > a) \quad \text{or} \quad y = -x \quad (x < a), \tag{6}$$

which provides a good approximation of the slowly varying parts. This function is represented by broken lines in Fig. 1(b). The slowly varying parts are linked by two fast transition layers located at $y = y_-$ and $y = y_+$, respectively.

The numerical solution suggests seeking a T-periodic solution that satisfies the antiphase condition

$$x_2(t - T/2) = x_1(t), \tag{7}$$

and admits a period close to twice the delay. To this end, we relate the period T and the delay τ as

$$T = 2\tau + 2\varepsilon\,\delta(\varepsilon), \tag{8}$$

where $\delta = O(1)$ as $\varepsilon \to 0$ needs to be determined. In order to describe the limit cycle, we first look for an approximation of the solution when it is a slowly varying function of t, i.e., when y is increasing from y_- to y_+ ($x > a$) and when y is decreasing from y_+ to y_- ($x < a$). We then examine the transition layers characterized by almost constant values of y (y_- or y_+), and by x function of the fast time t/ε.

A. Slowly varying parts

We start with Eqs. (4) and (5), and use (7) and (8) by noting that

$$x_2(t - \tau) = x_2(t - T/2 + \varepsilon\delta) = x_1(t + \varepsilon\delta), \tag{9}$$

$$x_1(t - \tau) = x_1(t - T/2 + \varepsilon\delta) = x_2(t + \varepsilon\delta). \tag{10}$$

Setting $\varepsilon = 0$, the leading problem is then given by

$$-x - y + H(x - a) = 0, \tag{11}$$

$$\frac{dy}{dt} = x, \tag{12}$$

for either (x_1, y_1) or (x_2, y_2). We start at $y = y_-$ with $x > a$. From (11) and (12), we then have the following equations:

$$x = 1 - y \quad \text{and} \quad \frac{dy}{dt} = 1 - y. \tag{13}$$

The solution for y is

$$y = (y_- - 1)\exp(-t) + 1 \tag{14}$$

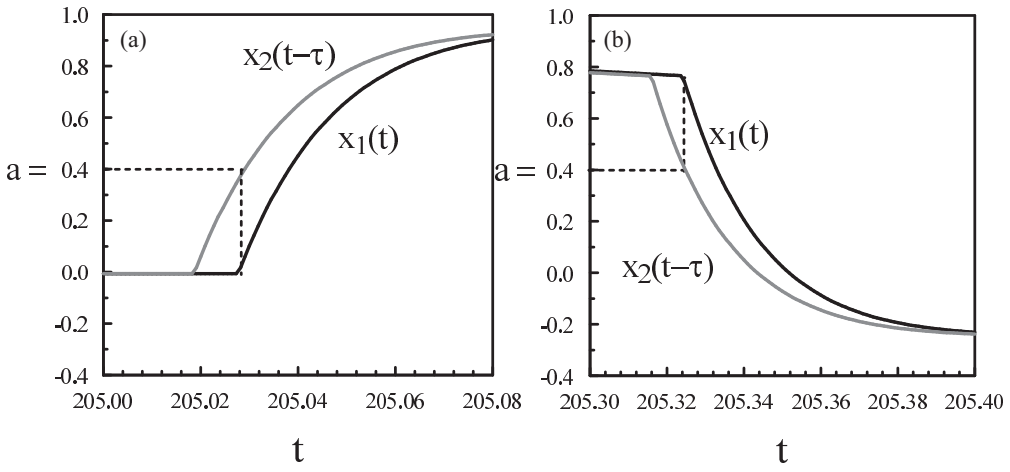

FIG. 2. Blowup of the fast transition layers of $x_1(t)$ when (a) $y \simeq y_-$ and when (b) $y \simeq y_+$. The figure also represents $x_2(t-\tau)$ which controls the Heaviside function.

and ends when $y = y_+$ at $t = t_+$. Using (14), we determine t_+ as

$$t_+ = \ln\left[\frac{y_- - 1}{y_+ - 1}\right]. \tag{15}$$

We next consider the slow evolution from $y = y_+$ at time $t = t_+$ with $x < a$. From (11) and (12), the evolution equations now are

$$x = -y \quad \text{and} \quad \frac{dy}{dt} = -y. \tag{16}$$

The solution for y is

$$y = y_+ \exp[-(t - t_+)] \tag{17}$$

and ends when $y = y_-$ at time $t = t_-$. From (17), we obtain $t_- - t_+$ as

$$t_- - t_+ = \ln\left(\frac{y_+}{y_-}\right). \tag{18}$$

Ignoring the contributions of the fast transition layers, the leading expression of the period T as $\varepsilon \to 0$ equals t_-. Using then (8), we conclude that $T = 2\tau$ equals t_-, in first approximation. Using (15) and (18), we obtain

$$T = \ln\left[\frac{y_- - 1}{y_+ - 1}\right] + \ln\left(\frac{y_+}{y_-}\right) = 2\tau. \tag{19}$$

This equation can be rewritten as

$$\left[\frac{y_- - 1}{y_+ - 1}\right]\left(\frac{y_+}{y_-}\right) = \exp(2\tau). \tag{20}$$

Equation (20) represents a first relation between the unknown y_- and y_+. We need a second equation for y_- and y_+, which motivates the analysis of the fast transition layers.

B. Transition layers

Figure 2 shows a blowup of the two fast transition layers for $x_1(t)$ and $x_2(t-\tau)$. In Fig. 2(a), y remains close to y_- and $x_1(t)$ increases following Eq. (4). The equation for x_1 can be rewritten as

$$\varepsilon\frac{dx_1}{dt} = -y_- - x_1 + H[x_2(t-\tau) - a]. \tag{21}$$

From Eq. (21), we note that an increase of x_1 is possible only if the Heaviside function takes its value 1. This occurs as soon as $x_2(t-\tau) > a$, which is what we observe numerically in Fig. 2(a). To properly formulate the transition layer equation, we introduce the fast time $s \equiv t/\varepsilon$ and note that

$$x_2(t-\tau) = x_2(t - T/2 + \varepsilon\delta) = x_1(t + \varepsilon\delta) = x_1(s + \delta), \tag{22}$$

which then implies using (21) that

$$\frac{dx_1}{ds} = -y_- - x_1 + H[x_1(s+\delta) - a]. \tag{23}$$

This equation must be solved with the conditions [see Fig. 3(a)]

$$x_1(0) = -y_- \quad \text{and} \quad x_1(\delta) = a. \tag{24}$$

Since $H[x_1(s+\delta) - a] = 1$ as soon as $s > 0$, Eq. (23) becomes ordinary and its solution is

$$x_1(s) = -\exp(-s) + 1 - y_-. \tag{25}$$

The condition $x_1(\delta) = a$ requires that

$$a = -\exp(-\delta) + 1 - y_-. \tag{26}$$

Figure 2(b) is a blowup of the fast transition where $y \simeq y_+$ and x_1 decreases from $x_1 = 1 - y_+$. Its fast change is now

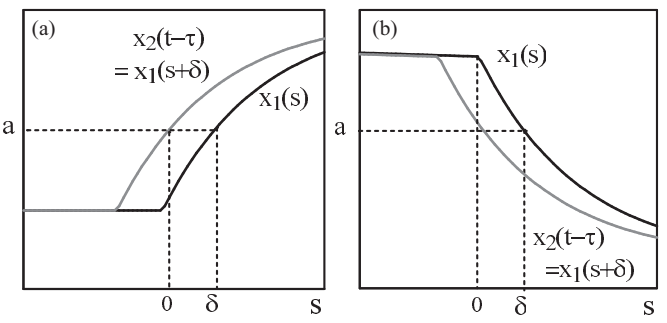

FIG. 3. Same transition layers as in Fig. 2 but in terms of the transition layer variable s. δ is defined as the interval of time between $x_2(t-\tau)$ and $x_1(t)$ when they are sequentially equal to a.

described by

$$\varepsilon \frac{dx_1}{dt} = -y_+ - x_1 + H[x_2(t-\tau) - a]. \tag{27}$$

The decrease of x_1 is possible only when $x_2(t-\tau) < a$ so that the Heaviside function is zero. This is indeed what we observe in Fig. 2(b). Mathematically, we introduce a new inner time variable defined as $s = (t - t_+)/\varepsilon$ and formulate the transition layer problem as [see Fig. 3(b)]

$$\frac{dx_1}{ds} = -y_+ - x_1 + H[x_1(s+\delta) - a], \tag{28}$$

$$x_1(0) = 1 - y_+ \quad \text{and} \quad x_1(\delta) = a. \tag{29}$$

Since $H[x_1(s+\delta) - a] = 0$ as soon as $s > 0$, Eq. (28) becomes ordinary and admits the solution

$$x = \exp(-s) - y_+. \tag{30}$$

The condition $x_1(\delta) = a$ then requires that

$$a = \exp(-\delta) - y_+. \tag{31}$$

Adding Eqs. (26) and (31), we obtain a second equation for y_- and y_+,

$$2a = 1 - y_- - y_+. \tag{32}$$

Using Eq. (20), we eliminate y_- and obtain

$$\frac{(-2a - y_+)}{(y_+ - 1)} \frac{y_+}{(1 - 2a - y_+)} = \exp(2\tau) \tag{33}$$

or, equivalently, a quadratic equation for y_+,

$$y_+^2[-1 + \exp(2\tau)] - 2y_+\{a[1 - \exp(2\tau)] + \exp(2\tau)\} + \exp(2\tau)(1 - 2a) = 0. \tag{34}$$

The solution of Eq. (34) with $y_+ < 1$ is shown in Fig. 4. y_- is then determined using (32), and δ is obtained using (31).

We note from Fig. 4(a) that y_+, y_-, and δ quickly approach constant values as τ is increased from zero. From (34), (32), and (31), we find the approximations

$$y_+ \simeq 1 - 2a, \quad y_- \simeq \frac{1 - 2a}{2a} \exp(-2\tau), \quad \text{and} \quad \delta \simeq -\ln(1 - a) \tag{35}$$

as $\exp(2\tau) \to \infty$. They are verified as soon as $\tau \geqslant 2$.

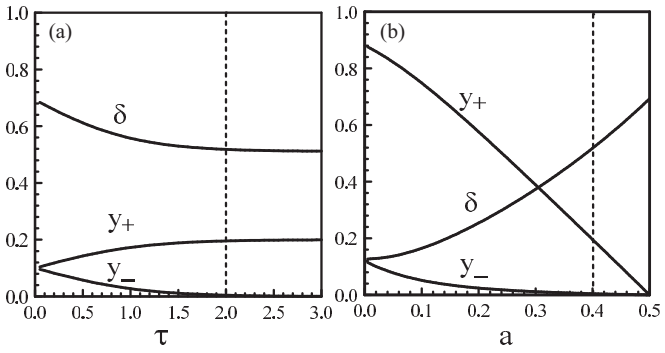

FIG. 4. Leading approximations of $y = y_\pm$ and δ. (a) $a = 0.4$; (b) $\tau = 2$. If $a = 0.4$ and $\tau = 2$, $y_- = 0.004$, $y_+ = 0.20$, and $\delta = 0.52$ (num: $y_- = 0.007$, $y_+ = 0.25$, and $\delta = 0.5$).

As $\tau \to 0$ [a fixed Fig. 4(a)] or as $a \to 1/2$ [τ fixed Fig. 4(b)], the difference $y_+ - y_-$ between the extrema of y decreases to zero and our analysis becomes invalid. A different analysis is required where either τ or $a - 1/2$ are scaled with respect to ε.

III. EXPERIMENTS

In order to test the experimental accessibility of our analytical results we have performed measurements on a nonlinear electronic circuit that simulate our FHN system (see Fig. 5). The circuit consists of several operational amplifiers (two acting as integrators, two as inverters) with associated feedback components. The voltages V_x and V_y are the dependent variables; $V_z = V_z(V_x)$ provides the Heaviside nonlinearity by using U_{1a} and $Q1$. The evolution equations for V_x and V_y are given by

$$R_2C_2 \frac{dV_x}{dT} = -V_x - V_y - V_z + 3V_{\text{ref}}, \tag{36}$$

$$\frac{dV_y}{dT} = \frac{V_x}{R_4C_4} - \frac{V_{\text{ref}}}{R_4C_4} + \frac{V_{\text{ref}}}{R_5C_4} - \frac{V_y}{R_5C_4}, \tag{37}$$

while

$$V_z = -V_{\text{ref}} H[V_x(T - T_D) - V_a] + V_{\text{ref}}. \tag{38}$$

The circuit was built twice on a "breadboard" and connected to a microcontroller based delay, built around an OLIMEX SAM7LA2 board. The board is connected to a PC host via RS232 and outfitted with 12-bit digital-to-analog (DA) converters. For analog-to-digital (AD), the microcontrollers 10-bit internal AD converters were used.

We next reformulate Eqs. (36)–(38) in dimensionless form. All AD/DA converters have a voltage range between 0 V and 2.5 V. $V_{\text{ref}} = 1.25$ V and 1.25 V $< V_a <$ 1.875 V are generated by a DA output which allows us to use V_a as a control parameter. Introducing the new variables x, y, z, s, and parameter a as

$$x, y, z = \frac{V_{x,y,z} - V_{\text{ref}}}{V_{\text{ref}}}, \quad t = T/(R_4C_4), \quad \text{and} \quad a = \frac{V_a - V_{\text{ref}}}{V_{\text{ref}}}$$

into Eqs. (36)–(38), we obtain

$$\varepsilon \frac{dx}{dt} = -x - y + H[x(t-\tau) - a], \tag{39}$$

$$\frac{dy}{dt} = x - y\frac{R_4}{R_5}, \tag{40}$$

where

$$\varepsilon = \frac{R_2C_2}{R_4C_4}.$$

The ration $R_4/R_5 = 0.013$ is small which motivates the elimination of the last term in Eq. (40). Equations (39) and (40) then have the same form as Eqs. (4) and (5). The choice of $R_4C_4 \simeq 100$ ms and $R_2C_2 \simeq 2$ ms implies $\varepsilon = 0.02$. The microcontroller is programed to sample at $T_s = 200$ μs and the delay is $T_D = 10^3 T_s = 200$ μs. This then leads to $\tau = T_D/(R_4C_4) = 2$.

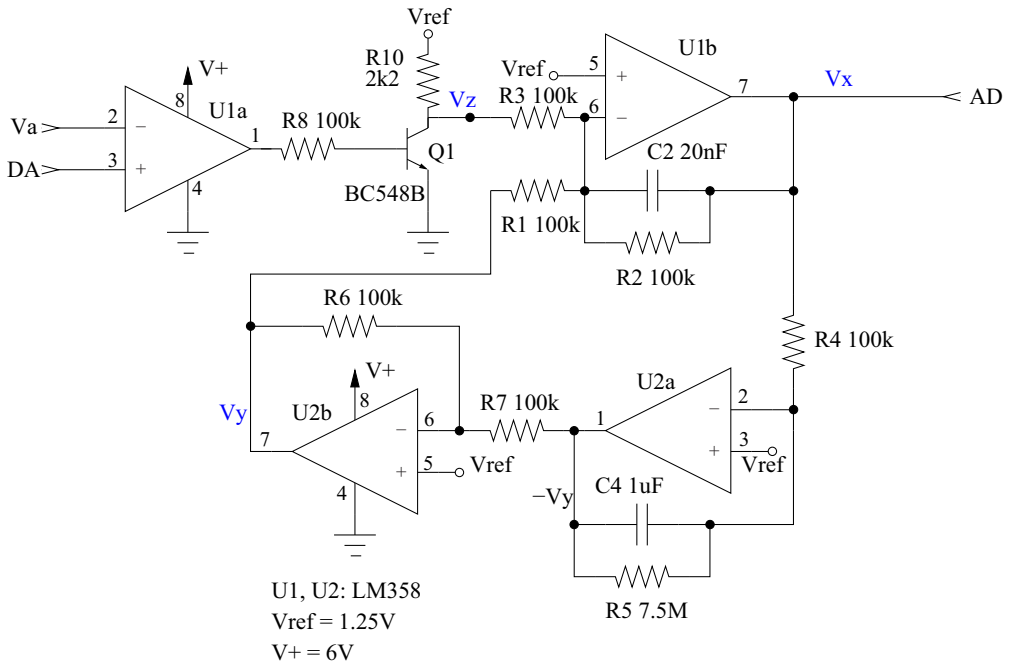

FIG. 5. (Color online) FHN circuit. U_{1a} is used as a comparator to build the Heaviside step function. The delay is built using a microcontroller with AD and DA converters (not shown).

Component variations are causing systematic errors which are important as we determine the small correction of the period given by $\varepsilon\delta$. Consequently, all operating components were carefully measured and the length of the delay lines were adjusted to keep τ and ε as close as possible to their fixed values $\tau = 2$ and $\varepsilon = 0.02$. The control parameter a was gradually changed from $a = 0.015$ to 0.45. At the beginning of each experiment, one of the two delay lines was loaded with a pulse so that the stable rest state is strongly perturbed and a periodic wave is initiated. For each value of a, the experiment was run for an interval of time of 700τ. The contents of the delay lines were then transferred to the host PC before we change the value of a. The values of V_y were also recorded and lead to the experimental bifurcation in Fig. 6. Compared to Fig. 4(b), we observe a good quantitative agreement between analytical and experimental bifurcation diagrams.

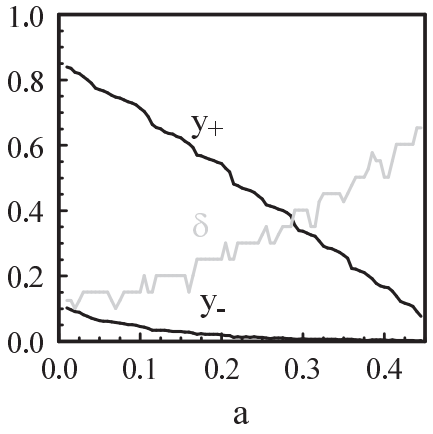

FIG. 6. Experimental bifurcation diagram with a as the bifurcation parameter.

IV. DISCUSSION

We performed an analytical study of a stable periodic solution of two mutually delay-coupled FHN systems. This solution coexists with a stable steady state and its existence cannot be anticipated from a linear stability analysis of a basic steady state. Indeed, this periodic regime emerges from a limit point (saddle node) of limit cycles and we believe that this bifurcation mechanism is important for problems modeled by delay differential equations. Another case of isolated branches of periodic solutions is documented for a laser subject to a delayed feedback [15]. In order to observe these oscillations experimentally, we built a system of two coupled electronic circuits that is described mathematically by the same FHN equations. Despite the difficulty measuring the small correction to the leading approximation of the period, we obtain quantitative agreement between analytical and experimental bifurcation diagrams.

The delay-induced branching of periodic solutions is possible because of a perfect synchronization between the current and delayed fast pulses in x_1 and x_2. The time history of the fast transition layers plays an active role in the determination of the bifurcation equations. For opto-electronic oscillators exhibiting slow-fast square-wave oscillations, a similar asymptotic analysis of a limit-cycle solution was possible [18,19]. However, the analysis of the fast transition layers is not needed for the derivation of the bifurcation equations. For these optoelectronic oscillators, the square-wave oscillations result from a Hopf bifurcation mechanism.

We concentrated on the case where the two coupled units oscillate in antiphase with a period close to twice the delay. But stable in-phase periodic solutions with a period close to the delay have also been observed. The asymptotic analysis of this case leads to Eqs. (31) and (32), and the following

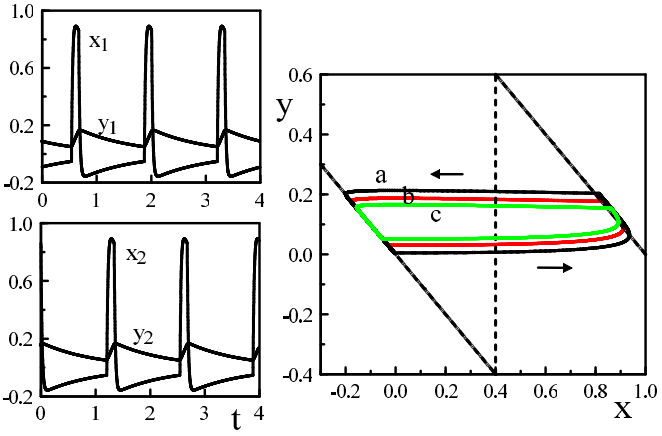

FIG. 7. (Color online) (Left) $2\tau/3$-periodic oscillations in antiphase. The values of the parameters are $a = 0.4$, $\varepsilon = 0.02$, and $\tau = 2$. (Right) Three distinct periodic regimes coexist with the stable steady state: (a) oscillations in antiphase with a period close to 2τ ($T = 4.021$), (b) oscillations in phase with a period close to τ ($T = 2.012$), and (c) oscillations in antiphase with a period close to $2\tau/3$ ($T = 1.342$).

equation for the maximum y_+:

$$y_+^2[-1 + \exp(\tau)] - 2y_+\{a[1 - \exp(\tau)] + \exp(\tau)\} + \exp(\tau)(1 - 2a) = 0. \quad (41)$$

If $\exp(\tau)$ is sufficiently large, we obtain the same bifurcation diagram as for the antiphase periodic solution. Furthermore, a stable antiphase of period close to $2\tau/3$ was also found numerically. See Fig. 7. We note that the orbits of the τ and $2\tau/3$-periodic regimes are smaller in amplitude compared to the 2τ-periodic solution suggesting that they could be less robust with respect to noise. This question is currently investigated experimentally by using our electronic system.

The asymptotic analysis is based on the limit ε small which allows us to find separate approximations for the slow and fast evolutions of the solution. These approximations are valid provided the difference $y_+ - y_-$ remains $O(1)$ compared to ε. The limit point of periodic solutions is located at $\tau = 0$ [Fig. 4(a)] or at $a = 1/2$ [Fig. 4(b)], in first approximation. If $y_+ - y_- \to 0$, a different analysis is needed where either τ or $a - 1/2$ is scaled with respect to ε.

We have verified that all the periodic solutions constructed or simulated numerically using the piecewise linear FHN equations (4) and (5) can be observed numerically for the continuous FHN equations (1) and (2). Figure 4, however, indicates that the limit cycle never reaches the extrema of the Z-shaped nullcline. This contrasts with the continuous FHN system where the limit cycle may come close to the extrema of the S-shaped nullcline [11]. If the delay is sufficiently large, the time evolution along the left branch of the S-shaped nullcline becomes longer, spending a lot of time near the stable steady state before jumping to the right branch. This provides the value of y_0 in Eq. (3) as being the steady-state value. However, the time lag δ is still unknown and the solution of the transition layer equation (3) is still an open problem. In [11], the transition layer is treated as an initial value problem that is solved with several assumptions.

Finally, we note that the case of two distinct delays [$x_2(t - \tau_2)$ and $x_1(t - \tau_1)$ in Eq. (1)] can be reduced to the problem of identical delays by reformulating the evolution equations [20]. In addition, the synchronization problem with both delayed coupling and delayed self-feedbacks has also been explored [21].

ACKNOWLEDGMENTS

T.E. is grateful for the invitations of Eckehard Schöll to visit his group at the TU Berlin. He also thanks Markus Dahlem for many stimulating discussions. T.E. and L.W. acknowledge the support of the F.N.R.S. (Belgium) and the Belgian F.R.I.A. for a Ph.D. scholarship, respectively. This work benefited from the support of the Belgian Science Policy Office under Grant No. IAP-7/35 "photonics@be."

[1] L. Glass, in *The Handbook of Brain Theory and Neural Networks*, 2nd ed., edited by M. A. Arbib (MIT Press, Cambridge, MA, 2003), p. 205; M. I. Rabinovich and H. D. I. Abarbanel, Neuroscience **87**, 5 (1998).

[2] C. M. Gray, J. Comput. Neurosci. **1**, 11 (1994); M. Meister, Science **252**, 939 (1991).

[3] R. M. Harris-Warrick *et al.*, in *Dynamic Biological Networks: The Stomatogastric Nervous System*, edited by R. M. Harris-Warrick *et al.* (MIT Press, Cambridge, MA, 1992).

[4] J. Keener and J. Sneyd, *Mathematical Physiology*, Interdisciplinary Mathematics (Springer-Verlag, New York, 1998).

[5] *Computational Cell Biology*, edited by C. P. Fall, E. S. Marland, J. M. Wagner, and J. J. Tyson (Springer-Verlag, New York, 2002).

[6] G. Bard Ermentrout and David H. Terman, *Mathematical Foundations of Neuroscience*, Interdisciplinary Applied Mathematics Vol. 35 (Springer, New York, 2010).

[7] S. A. Campbell, in *Handbook of Brain Connectivity*, edited by V. K. Jirsa and A. R. McIntosh (Springer, New York, 2007), pp. 65–89.

[8] G. Stepan, Philos. Trans. R. Soc. A **367**, 1059 (2009).

[9] N. Buric and D. Todorovic, Phys. Rev. E **67**, 066222 (2003).

[10] M. A. Dahlem, G. Hiller, A. Panchuk, and E. Schöll, Int. J. Bifurcat. Chaos **19**, 745 (2009).

[11] E. Schöll, G. Hiller, P. Hövel, and M. A. Dahlem, Philos. Trans. R. Soc. A **367**, 1079 (2009).

[12] O. Vallès-Codina, R. Möbius, S. Rüdiger, and L. Schimansky-Geier, Phys. Rev. E **83**, 036209 (2011).

[13] T. Prager, H.-P. Lerch, L. Schimansky-Geier, and E. Schöll, J. Phys. A: Math. Theor. **40**, 11045 (2007).

[14] S. Rüdiger and L. Schimansky-Geier, J. Theor. Biol. **259**, 96 (2009).

[15] T. Erneux, *Applied Delay Differential Equations* (Springer, Berlin, 2009), Chap. 7.

[16] S. Coombes and C. R. Laing, Philos. Trans. R. Soc. A **367**, 1117 (2009).

[17] S. Coombes and C. R. Laing, Physica D **238**, 264 (2009).

[18] L. Weicker, T. Erneux, O. d'Huys, J. Danckaert, M. Jacquot, Y. Chembo, and L. Larger, Phys. Rev. E **86**, 055201(R) (2012).

[19] L. Weicker, T. Erneux, O. d'Huys, J. Danckaert, M. Jacquot, Y. Chembo, and L. Larger, Philos. Trans. R. Soc. A **371**, 20120459 (2013).

[20] A. Panchuk, M. A. Dahlem, and E. Schöll, Proc. NDES **09**, 177 (2009), arXiv:0911.2071v1.

[21] A. Panchuk, D. P. Rosin, P. Hövel, and E. Schöll, Int. J. Bifurcat. Chaos **23**, 1330039 (2013).